Electric-Field-Effect Modulation of the Transition Temperature, Mobile Carrier Density, and In-Plane Penetration Depth of NdBa 2 Cu 3 O 7 − δ Thin Films

D. Matthey, N. Reyren, J.-M. Triscone, T. Schneider

Electric field effect modulation of transition temperature, mobile carrier density and in-plane penetration depth in $NdBa_2Cu_3O_{7-\delta}$ thin films

D. Matthey,* N. Reyren, and J.-M. Triscone
DPMC, University of Geneva, 24 quai Ernest-Ansermet, 1211 Geneva 4, Switzerland.

T. Schneider
Physikinstitut, University of Zurich, Winterthurerstrasse 190, 8057 Zurich, Switzerland.
(Dated: September 13, 2006)

We explore the relationship between the critical temperature, T_c, the mobile areal carrier density, n_{2D}, and the zero temperature magnetic in-plane penetration depth, $\lambda_{ab}(0)$, in very thin underdoped $NdBa_2Cu_3O_{7-\delta}$ films near the superconductor to insulator transition using the electric field effect technique. Having established consistency with a Kosterlitz-Thouless transition we observe that T_{KT} depends linearly on n_{2D}, the signature of a quantum superconductor to insulator transition in two dimensions with $z\overline{\nu} = 1$, where z is the dynamic and $\overline{\nu}$ the critical exponent of the in-plane correlation length.

PACS numbers: 71.30.+h, 74.78.Bz, 74.72.-h, 74.75.Ha

The electronic properties of high T_c superconductors are critically determined by the density of mobile holes as illustrated by their generic phase diagram in the temperature dopant concentration plane. Understanding the physics of this phase diagram, in particular at the two $T = 0$ edges of the superconducting dome, has emerged as one of the critical questions in the field of cuprate superconductors. In the underdoped regime, where a superconductor to insulator transition occurs, there is an empirical linear relation (the so-called Uemura relation) between T_c and $\lambda_{ab}^{-2}(0)$ [1], where λ_{ab} is the in-plane London penetration depth. If, in the underdoped limit, a two dimensional (2D) quantum superconductor to insulator (QSI) transition occurs, such a relation between T_c and $1/\lambda^2(0)$ is expected [2]. This however necessitates the occurrence of a 3D to 2D crossover as the underdoped limit is approached with a diverging anisotropy $\gamma = \lambda_c/\lambda_{ab}$. In the case of a 3D QSI-transition, one would expect $T_c \propto \lambda_{a,b,c}(0)^{-2z/(z+1)}$, where z is the dynamic critical exponent of the transition [2]. Recent penetration depth measurements on $YBa_2Cu_3O_{6+x}$ single crystals [3, 4] (where γ apparently saturates at low doping levels) and films [5] suggest a 3D-transition with $2z/(z+1) \simeq 1$ [6], a result different from the Uemura relation. Furthermore, an empirical relation involving the normal state conductivity and extending up to optimum doping was recently proposed by Homes *et al.* [7]. However, all these studies on the relationship between T_c and $\lambda_{a,b,c}(0)$ stem from samples where the doping level was modified by chemical substitution [1–8].

In this letter we use the electrostatic field effect to tune the mobile areal carrier density, n_{2D}, in ultrathin, strongly underdoped $NdBa_2Cu_3O_{7-\delta}$ (NBCO) films and explore the intrinsic relation between T_c, n_{2D} and $\lambda_{ab}^{-2}(0)$ close to the superconductor to insulator transition. The electrostatic field effect technique, which allows the carrier density in a given sample to be changed without affecting the chemical composition, thus avoiding sample to sample variations and substitution induced disorder, appears to be an ideal method to elucidate the intrinsic relationships between the key physical parameters [9].

In a classical oxide field effect configuration, an electric field is applied across a gate dielectric in a heterostructure made of an oxide channel and a dielectric layer. The density of carriers is modified at the interface between the oxide channel and the dielectric, changing the electronic properties of the oxide channel. This technique allows us to induce in thin oxide superconducting films rather large T_c modulations [10]. In the 3-4 unit cell thick films used in this study, T_c modulations of more than 10 K have been achieved, corresponding to induced charge densities of the order of $0.7 \cdot 10^{14}$ charges/cm^2.

The field effect device used in this study, described in Ref. 10, is based on a $SrTiO_3$ (STO) single crystal gate dielectric, the substrate itself. Due to its large low temperature dielectric constant, ε, and large achievable polarizations, STO is a particularly interesting gate insulator. Field effect devices using a STO thin film gate insulator have thus been studied extensively [11]. Here, thin 100 μm thick, or thinned 500 μm commercial substrates have been used. A sketch of the thinned device is shown in the upper inset of Fig.1. The superconducting NBCO thin films are first grown by off-axis magnetron sputtering onto (001) (bare or etched) STO substrates heated to about 730°C. During cooling, a typical O_2 pressure of 670 Torr is used to obtain optimally doped films. To control the initial doping level of the films, the oxygen cooling pressure is modified and lowered down to 5 mTorr for the most underdoped films. Gold is sputtered in-situ at room temperature to improve the contact resistances and the whole structure is protected by an amorphous NBCO layer also deposited in-situ. X-ray diffraction allowed us to determine precisely the film thickness down to three unit cell thick films. After deposition, the sam-

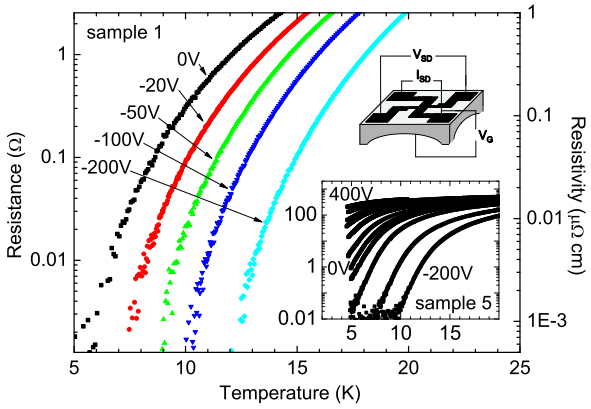

FIG. 1: Resistance versus temperature for a 3-4 unit cell thick NBCO film (sample 1) for different applied gate voltages; the right scale is the corresponding resistivity. The lower inset shows the resistance as a function of temperature for sample 5, which is also 3-4 unit cell thick, for different applied gate voltages (see text for details). The upper inset shows a sketch of the field effect device, based on a thinned STO single crystal gate insulator.

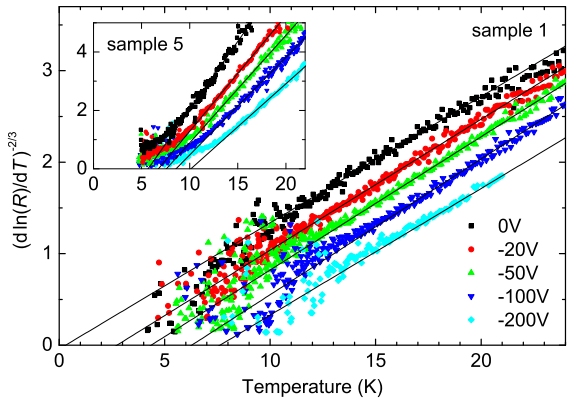

FIG. 2: $(\mathrm{d}\ln R/\mathrm{d}T)^{-2/3}$ *vs.* T for samples 1 and 5 at various gate voltages. The solid lines indicate the consistency with the linear KT relationship. $T_c = T_{KT}$ is determined by the condition $(\mathrm{d}\ln R/\mathrm{d}T)^{-2/3} = 0$ at T_{KT}.

ples are photolithographically patterned using ion milling and a gold electrode is deposited on the backside of the samples, facing the central part of the superconducting path. The measured path is 600 (length)×500 (width) μm^2. The patterning process does not affect T_c. All the thin films presented here are 3-4 unit cell thick.

Fig.1 shows resistance versus temperature for sample 1 in the tail of the transitions, for different voltages applied across the gate dielectric: 0, −20, −50, −100 and −200V. Negative voltages correspond to a negative potential applied to the gate and a positive one to the superconducting path, resulting in hole doping of the oxide channel and, as expected, in a "shift" to higher temperatures of the resistive transition. Resistance measurements are performed using a standard four point technique while a voltage, V_g, is applied to the gate. During measurements, gate leakage currents were kept below a few nA, while the current used for resistance measurements was typically between 1 and 10μA. The lower inset of Fig.1 shows resistance versus temperature for sample 5 and for gate voltages of 400, 200, 100, 50, 20, 10, 0, −5, −20 , −50, −100, and −200 V. At 4.2K, a large increase in resistance is observed while applying positive gate voltages, effectively reducing the hole concentration.

To estimate T_c, we explore the consistency of our resistivity data with the expected behavior for a Kosterlitz-Thouless (KT) transition, namely $\rho = \rho_0 \exp(-bt^{-1/2})$, where $t = T/T_c - 1$ and ρ_0 and b are material dependent but temperature independent parameters [2]. Accordingly, consistency with the KT-scenario is established when the plot $(\mathrm{d}\ln R/\mathrm{d}T)^{-2/3}$ *vs.* t exhibits, near $t = 0$, linear behavior and $T_c = T_{KT}$ is determined by the condition $(\mathrm{d}\ln R/\mathrm{d}T)^{-2/3} = 0$ at T_{KT}. A glance at Fig.2 reveals that the characteristic KT-behavior is well confirmed in an intermediate regime. In sample 1, it is the noise level which limits the accessible regime, while in sample 5 a rounded transition appears to occur, a signature that the correlation length divergence is limited by the size of the homogenous domains. Indeed, above T_{KT} the correlation length increases exponentially as $\xi = \xi_0 \exp(bt^{-1/2})$. An estimate of the size of the homogeneous regions for sample 5 for $T \simeq 7.5$K, $T_{KT} = 5.67$K and $b = 2.63$ (values appropriate for sample 5 at $V = 0$), leads to $\xi\,(7.5\mathrm{K})\,/\xi_0 \simeq 100$. Remarkably enough, with ξ_0 ranging from 10 to 100Å, the size of the homogeneous domains exceeds 1000Å.

The consistency with a KT-transition discussed above enables us to estimate $T_c = T_{KT}$ and determine its gate-voltage dependence. The resulting T_{KT} estimates for various samples versus gate voltage V are plotted in Fig.3a. As can be seen, $T_{KT}\,(V)$ is nonlinear and, as indicated by the respective solid curves, $T_{KT}\,(V) \simeq T_{KT}\,(0) + a\,|V|^{1/2}$.

To correlate the field-induced T_{KT} modulations to the field-induced areal carrier density, $n_{2\mathrm{D}}$, we measured the accumulated charge Q. Since the dielectric constant of STO depends on temperature and applied electric field, we measured the field and temperature dependence of the capacitance [12]. The induced areal charge density, $\sigma = e\Delta n_{2\mathrm{D}}$, at a given temperature was measured in terms of the capacitance of the device as a function of the applied gate voltage, using an LCR meter (Agilent 4284A) with an auto-balancing bridge method, and/or by measuring the charge flow during loading using an electrometer (Keithley 6514). By ramping the voltage across the dielectric, the LCR-meter measures the "local" ca-

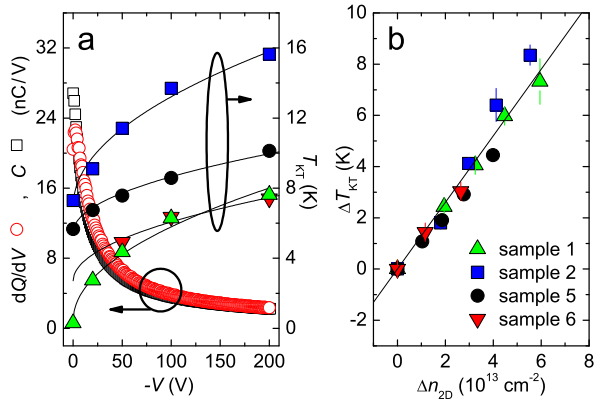

FIG. 3: (a) Right scale, T_{KT} versus gate voltage V. The solid lines are $T_{KT}(V) \simeq T_{KT}(0) + a|V|^{1/2}$ with $a = 0.54$, 0.62, 0.32, 0.34 for samples 1, 2, 5 and 6. Left scale, $\mathrm{d}Q/\mathrm{d}V$ versus V for a 100μm thick STO measured at 4.2 K using an electrometer (open circles), $C(V)$ measured using an LCR-meter (open squares). (b) ΔT_{KT} *vs.* Δn_{2D} for all the samples. The solid line is Eq.(1).

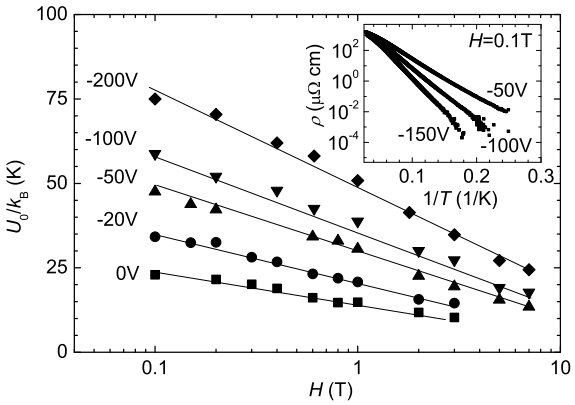

FIG. 4: U_0/k_B *vs.* H for different applied voltages for sample 1. A linear relation between U_0 and $\log(H)$ is observed with a slope which depends on the applied electric field. Inset: $\log(\rho)$ as a function of $1/T$ for sample 2 and for three different electrical fields at 0.1T. The zero temperature activation energy U_0 at a given applied electrical field is obtained from the slope of the Arrhenius plot.

pacitance $C(V)$ at a given voltage while the electrometer measures $\mathrm{d}Q$ for a given change in voltage [27]. The two measurements agree quantitatively as can be seen on Fig.3a where $\mathrm{d}Q/\mathrm{d}V$ and $C(V)$ ($\mathrm{d}Q = C(V)\mathrm{d}V$), measured at 4.2K, are plotted versus V for a 100μm thick STO substrate with two parallel 20 mm^2 square gold electrodes. The corresponding field induced charge density $\sigma(V)$ at a given voltage and temperature is then obtained from $\sigma(V) = 1/S \int_0^V C(V)\mathrm{d}V$, where S is the surface of the gate contact. This quantitative estimate of σ allows a change in T_{KT} to be related to a change in the areal carrier density $n_{2D} = \sigma/e$. The result shown in Fig.3b reveals the intrinsic linear relationship

$$\Delta T_{KT} = 1.3\ 10^{-13} \Delta n_{2D}, \qquad (1)$$

where $\Delta T_{KT} = T_{KT}(V) - T_{KT}(0)$ [28] and Δn_{2D} is expressed in cm^{-2}. This is a novel and central result of our paper.

Together with the quantum counterpart of the Nelson-Kosterlitz relation [13], $T_{KT} \propto \lambda_{ab}^{-2}(T_{KT})$, it implies that T_{KT} , $\lambda_{ab}(0)$ and n_{2D} are universally related by

$$T_{KT} \propto n_{2D} \propto \frac{1}{\lambda_{ab}^2(0)}, \qquad (2)$$

with non-universal factors of proportionality. This relationship also confirms the theoretical predictions for a 2D-QSI transition. Indeed, the scaling theory of quantum critical phenomena [2, 16] predicts that close to a QSI transition T_c scales as $n_{2D}^{z\overline{\nu}}$, where z is the dynamic and $\overline{\nu}$ the critical exponent of the zero temperature in-plane correlation length, $\xi_{ab} \propto n_{2D}^{-\overline{\nu}}$. Thus, Eq.(2) reveals that $z\overline{\nu} \simeq 1$, the signature of a QSI transition in 2D [14, 15]. Since close to a QSI transition $\lambda_{ab}(0)$ scales as $1/\lambda_{ab}^2(0) \propto n_{2D}^{\overline{\nu}(D+z-2))}$ (D is the system dimensionality) [2, 16], it follows that $\Delta T_{KT} \propto \Delta n_{2D}$ does not only uncover a 2D-QSI transition with $z\overline{\nu} \simeq 1$, but also implies that T_{KT} , $\lambda_{ab}(0)$ and n_{2D} are universally related by Eq.(2). However, this relationship differs drastically from $T_c \propto 1/\lambda_{a,b,c}(0)$, derived from penetration depth measurements on $YBa_2Cu_3O_{6+x}$ single crystals [3, 4] and films [5], where T_c was reduced by chemical substitution.

To substantiate our main result further, we explore the temperature, electric and magnetic field dependence of the resistive transition, extracting the activation energy, U, for vortex motion in the liquid vortex phase. In the vortex 2D-limit the resistance in a field is activated with activation energy proportional to $-\ln(H)$. The measurements have been performed with the magnetic field applied perpendicular to the ab-plane, ramping the temperature slowly and measuring the sample resistance at a given magnetic and electric field. Inset of Fig.4 shows Arrhenius plots of the resistivity, $\log(\rho)$ as a function of $1/T$, for sample 2 and for three different electrical fields at $H = 0.1$T. The observed linear relation between $\log(\rho)$ and $1/T$ singles out thermally activated flux flow, where $\rho(H,T) = \rho_n \exp(-U(H,T)/k_BT)$, with $U(H,T) = 2U_0(H)(1 - T/T_c)$ for $T \sim T_c$ [17]. As can be seen, U becomes larger for electrical fields raising the number of holes and T_c. We note that an electrostatic modulation of the activation energies was also observed in reference 18. From such Arrhenius plots we estimated $U_0(H)/k_B$ for sample 1 at different applied voltages and different magnetic fields. As can be seen in Fig.4, at a given voltage, we observe between 0.1

and 7 T the characteristic 2D logarithmic field dependence $U_0(H) = -\alpha \ln(H) + \beta$, in agreement with previous measurements on thin films, superlattices, and the highly anisotropic kappa-(BEDT-TTF)$_2$Cu(NCS)$_2$ [19–24]. Note that in 3D $U \propto H^{-1/2}$ is expected [26]. Furthermore we find that $T_c = T_{KT}$ is proportional to $U_0(H)/k_B$ for every value of the magnetic field. Since U is proportional to $1/\lambda_{ab}^2$ in $D = 2$ (and $D = 3$) [25, 26], this proportionality is also consistent with our main result $T_c \propto n_{2D} \propto 1/\lambda_{ab}^2(0)$.

In summary, we explored the relationships between T_c, the mobile areal carrier density, $n_{2\mathrm{D}}$, and the zero temperature in-plane penetration depth, $\lambda_{ab}(0)$, for very thin underdoped NBCO films near the superconductor to insulator transition by means of the electric field effect technique. Together with the observed behavior of the resistive transition we established remarkable consistency with 2D critical behavior and a quantum superconductor to insulator transition, characterized by a linear relationship between T_c, $n_{2\mathrm{D}}$ and $1/\lambda_{ab}^2(0)$. This result also implies that isotope or pressure effects on T_c, $n_{2\mathrm{D}}$ and $\lambda_{ab}(0)$ are related accordingly.

We would like to thank P. Martinoli and S. Gariglio for useful discussions and M. Dawber for a careful reading of the manuscript. This work was supported by the Swiss National Science Foundation through the National Center of Competence in Research, "Materials with Novel Electronic Properties, MaNEP" and division II, New Energy and Industrial Technology Development Organization (NEDO) of Japan, and ESF (Thiox).

* Now at Department of Physics and Astronomy, University of Aarhus, Ny Munkegade, Building 1520, DK-8000 Aarhus C; Electronic address: daniel@inano.dk

[1] Y. J. Uemura *et al.*, Phys. Rev. Lett.**62**, 2317 (1989).
[2] T. Schneider and J. M. Singer *in Phase Transition Approach to High Temperature Superconductivity* (Imperial College Press, London, 2000).
[3] A. Hosseini *et al.*, Phys. Rev. Lett. **93**, 107003 (2004).
[4] D. M.Broun *et al.*, cond-mat/0509223.
[5] Y. Zuev *et al.*, Phys. Rev. Lett. **95**,137002 (2005).
[6] T. Schneider, cond-mat/0509768.
[7] C. C. Homes *et al.*, Nature **430**, 539(2004).
[8] J. L. Tallon *et al.*, Phys. Rev. B **68**, 180501(R) (2003).
[9] C. H. Ahn *et al.*, Nature **424**, 1015 (2003).
[10] D. Matthey *et al.*, Appl. Phys. Lett. **83**, 3758 (2003).
[11] J. Mannhart, Supercond. Sci. Technol. **9**, 49(1996).
[12] H.-M. Christen *et al.*, Phys. Rev. B **49**, 12095 (1994), A. Bhattacharya *et al.*, Appl. Phys. Lett. **85**, 997 (2004).
[13] D. R. Nelson and J. M. Kosterlitz, Phys. Rev. Lett. **39**, 1201 (1977).
[14] I. F. Herbut, Phys. Rev. B **61**, 14723 (2000).
[15] I. F. Herbut, Phys. Rev. Lett. **87**, 137004 (2001).
[16] K. Kim *et al.*, Phys. Rev. B **43**, 13583 (1991).
[17] T. T. M. Palstra *et al.*, Phys. Rev. B **41**, 6621 (1990).
[18] A. Walkenhorst *et al.*, Phys. Rev. Lett. **69**, 2709 (1992).
[19] O. Brunner *et al.*, Phys. Rev. Lett. **67**, 1354 (1991).
[20] Ø Fischer *et al.*, Physica Scripta **T42**, 46 (1992).
[21] W.R. White, A. Kapitulnik, M.R. Beasley, Phys. Rev. Lett. **70**, 670 (1993).
[22] Y. Suzuki, J.-M. Triscone, C.B. Eom, T.H. Geballe, Phys. Rev. Lett. **73**, 328 (1994).
[23] S. Friemel and C. Pasquier, Phys. C **265**, 121 (1996).
[24] X. Zhang, S.J. Wang, C.K. Ong, Phys. C **329**, 279-284 (2000).
[25] M. V. Feigel'man *et al.*, Phys. C **167**, 177 (1990).
[26] G. Blatter *et al.*, Rev. Mod. Phys. 66, 4, 1248 (1994).
[27] dQ is obtained for a dV of 1V. Also $C(V)$ was measured with voltage modulation amplitudes between 0.1 and 1V.
[28] Except for sample 6 where $\Delta T_{KT} = T_{KT}(V) - T_{KT}(-50\mathrm{V})$.

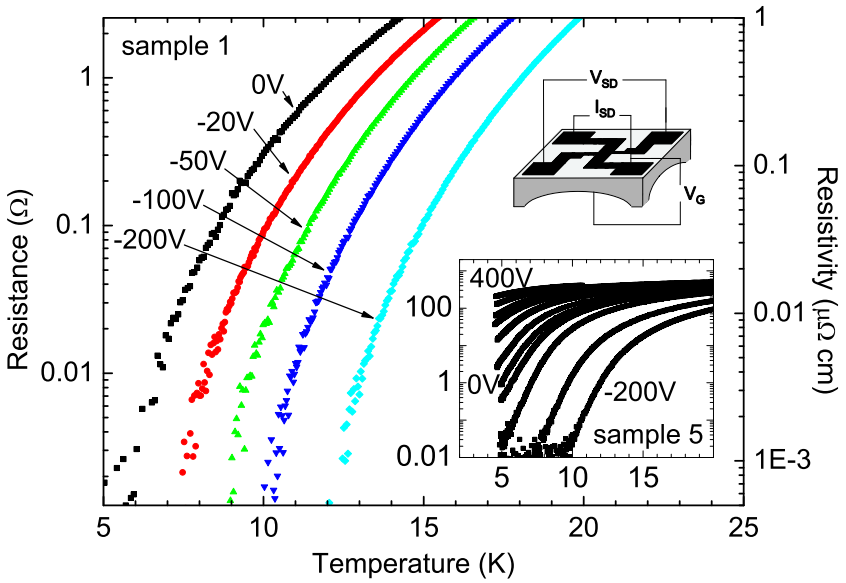
sample 1
0V
-20V
-50V
-100V
-200V
V_{SD}
I_{SD}
V_G
400V
0V
-200V
sample 5
Resistance (Ω)
Resistivity (μΩ cm)
Temperature (K)

Figure 1

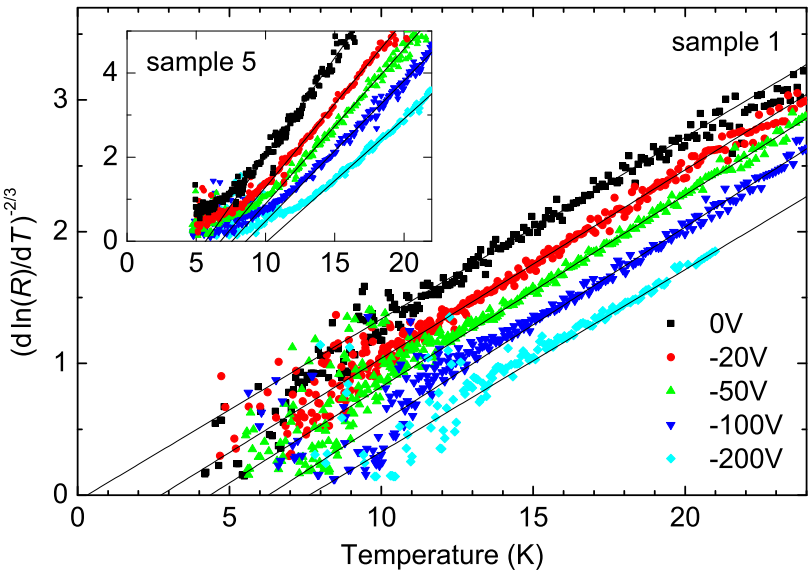
sample 1
sample 5
0V
-20V
-50V
-100V
-200V
(d ln(R)/dT)^-2/3
Temperature (K)
0
1
2
3
0
5
10
15
20
0
2
4

Figure 2

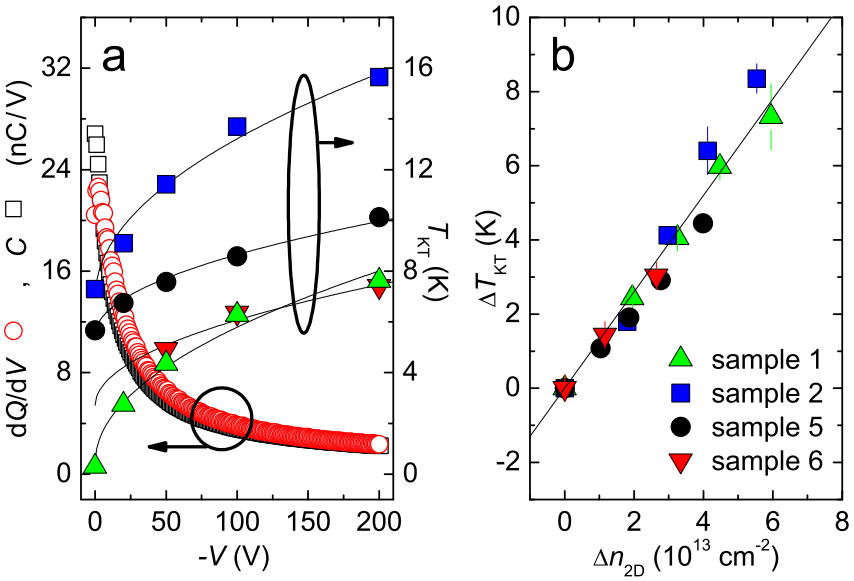
a
b
dQ/dV ○ , C □ (nC/V)
T_{KT} (K)
-V (V)
ΔT_{KT} (K)
Δn_{2D} (10^{13} cm^{-2})
sample 1
sample 2
sample 5
sample 6

Figure 3

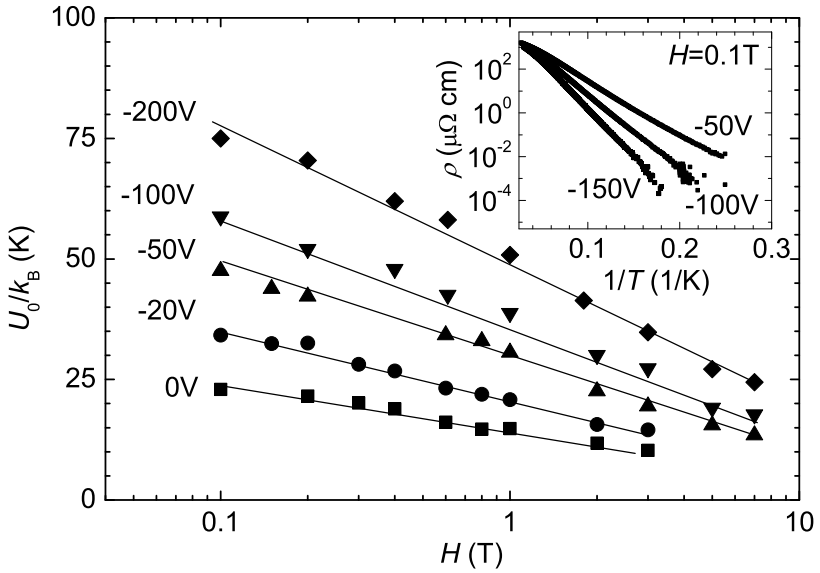
100
75
50
25
0
0.1
1
10
U_0/k_B (K)
H (T)
-200V
-100V
-50V
-20V
0V
H=0.1T
ρ (μΩ cm)
10^2
10^0
10^{-2}
10^{-4}
-50V
-150V
-100V
0.1
0.2
0.3
1/T (1/K)

Figure 4